OPEN ACCESS Freely available online

ISSN: 2252-5211
International Journal of Waste Resources

Research Article

Design and Characterization of Porous Geopolymer for Dye Removal

Elton Yerima Ngu[1*], Julson Aymard Tchio[1,2], Linda Lekuna Duna[2], Cyriaque Rodrigue Kaze[2], Elie Kamseu[2], Tchakoute Kouamo Herve[1], Cristina Leonelli[3]

[1]Department of Physical Chemistry and Applied Analysis, University of Yaounde, Soa, Cameroon; [2]Department of Environmental Sciences, University of Yaounde, Yaounde, Cameroon; [3]Department of Engineering Enzo Ferrari, University of Modena and Reggio Emilia, Modena, Italy

ABSTRACT

This study demonstrates the preparation of porous geopolymers using different foaming agents for dye removal in water using methylene blue as the model solution. The porous membranes were prepared by combining alkaline activation solution, aluminosilicate source (either clay-rich laterite or iron-rich laterite), amorphous silica (rice husk ash) with direct foaming (with either H_2O_2 or Al powder), followed by curing first at room temperature for two hours, then at 65°C for another two hours. The physical properties such as apparent porosity, bulk density, water absorption and stability in water were obtained to select porous geopolymer suitable for filtration. Results shows that the best porous geopolymer suitable for filtration were those prepared using hydrogen peroxide as foaming agent and have a rice husk content of ≤ 20%. Permeability test carried out on the selected foams revealed that they were not permeable, so there was need to optimize the foams. Three different surfactants were used for the optimization (stabilization) of the foams. Based on screening through permeability tests, the triton H66 surfactant was selected for use. The physical properties of the optimized selected foams showed an augmentation of these properties for a foam. This augmentation was seen to be influenced by the rice husk ash content in the matrices, with the augmentation increasing with rice husk ash content. Two optimized samples (one from each base material) was applied in methylene blue removal in a filtration column experiment. After 8 hours of collecting effluent, it exhibited a removal efficiency of approximately 97%. This efficiency reduced to 95% with the rice husk ash content of over 20% in the matrices. The membranes methylene blue removal potential was determine with an infrared spectroscopic analysis. The new peak at 395 cm^{-1} affiliated to C-N-C of methylene blue confirms the presence of adsorbed methylene blue in the matrices. The results obtained demonstrates that porous filters in this study can be potentially used in industrial and domestic wastewater treatment.

Keywords: Aluminum powder; Hydrogen peroxide; Foaming agent; Filter design; Methylene blue; Wastewater treatment

INTRODUCTION

Global development has led to a positive impact on factors like population growth, industrialization and urbanization. Increase in these factors entailed a huge demand and use of water. As a result, default amount of wastewater is being produced which if discarded directly into the environment, pollutants will accumulate which will become detrimental to life as we know it [1]. In order to prevent this, the wastewater needs to be treated before discarded in to the environment. To achieve this, several materials and cost effective methods has been applied to realize this treatment to disposable standards. Materials scientifically

Correspondence to: Elton Yerima Ngu, Department of Physical Chemistry and Applied Analysis, University of Yaounde, Soa, Cameroon, Tel: 670803969; E-mail: nguyerims@gmail.com

Received: 19-Nov-2022, Manuscript No. IJWR-22-18853; **Editor assigned:** 22-Nov-2022, PreQC No. IJWR-22-18853 (PQ); **Reviewed:** 06-Dec-2022, QC No. IJWR-22-18853; **Revised:** 23-Feb-2023, Manuscript No. IJWR-22-18853 (R); **Published:** 02-Mar-2023, DOI: 10.35248/2252-5211.23.13.522

Citation: Ngu EY, Tchio JA, Duna LL, Kaze CR, Kamseu E, Herve TK, et al. (2023) Design and Characterization of Porous Geopolymer for Dye Removal. Int J Waste Resour. 13:522.

exploited for this purpose include; sand, activated carbon, ceramics, geopolymers of which this paper draws interest to the application of porous geopolymer for wastewater treatment [2].

Geopolymers represent inorganic polymers with constituents, SiO_4 and AlO_4 tetrahedral as their structural units. They are usually prepared by means of a reaction between an aluminosilicate source (precursor) and a high pH alkali solution (activator). Due to their attractive properties like high mechanical strength, chemical attack stability, insulating properties etc, their application has become extensive in which wastewater treatment by filtration is a point of interest in this study. The application of geopolymer for wastewater treatment was first initiated with the conventional geopolymers, followed by porous geopolymer [3]. They were applied as adsorbents in both solid and powder form and were observed to have a high adsorption capacity for methylene blue dye, Cu^{2+}, Pb^{2+}, Cu^{2+}, Cr^{3+} and $Cd^{2+}$of which the most efficient results obtained was from porous geopolymer using precursors. This was attributed to the fact that apart from the ion exchange site found in the materials responsible for adsorption, porosity is also one of the components governing adsorption capacity of geopolymers [4].

Porous geopolymer can be prepared using 2 methods; the first is the mechanical foaming method through which the alkaline activated paste is mixed pre-developed foam or only the paste is mixed vigorously to introduce air into it. The second method which is the easiest, is the formation of pores by chemical foaming method (direct foaming method) by which the introduction of a blowing agent initiates a reaction, producing gas which are trapped in the matrix producing pores. Blowing agents often used are metal powder (Al, Si and Zn powder) or Hydrogen Peroxide (H_2O_2). The application of these porous geopolymers for wastewater filtration did not show promising results. This due to the formation of closed pore systems which makes them water impermeable [5]. There was need to optimize the foams to be applicable in water filtration. Surfactants were introduced into the geopolymer along with the blowing agent and were observed to produce open pores. Reason being that, the inclusion of surfactant led to the stabilization of the gas-liquid interface through the hindrance of bubble coalescence, continuous Ostwald ripening or spontaneous drainage. This set the foundation for the application of chemically induced porous geopolymer for filtration of water. The potential of these porous geopolymer to treat wastewater as both adsorbent and membrane gave an efficiency of up to an average of 80% with the effort to attain a higher efficiency still being exploited. The application of porous geopolymer for wastewater treatment by filtration has been clearly established to work. However, the question remains, of all the foaming agents used to induce pores, which is most suitable to produce good pores to provide efficient filtration treatment of wastewater and what are some of the factors that can influence their properties [6]. This study therefore has the novelty to produce porous geopolymer from 2 different foaming agents to evaluate their suitability in water treatment.

In view of this background, the aim of this study was to carry out a comparative study on porous geopolymer produced using 2 different foaming agents with 2 different aluminosilicate precursors to evaluate which is suitable for wastewater treatment. Rice Husk Ash (RHA) was also used to vary the Si/Al ratio of the precursor to get different reaction mediums [7-10]. The produced geopolymer matrix were characterized using different techniques like the physical property (bulk density, apparent porosity and water absorption), Fourier Transformed Infrared Spectroscopy (FTIR), X-ray diffraction and Scanning Electron Microscopy (SEM). Selected geopolymer foams' potential to treat wastewater were obtained through the means of a filtration experiment in a filtration column and FTIR analysis carried out on the used matrices before and after treatment.

MATERIALS AND METHODS

Materials

In this study, the sources of aluminosilicate used were clay-rich laterite, obtained from Bamenda, Northwest region, and iron-rich laterite from Emana, Yaounde. The raw materials were oven dried at 120°C for 24 hours, grounded to a particle size of 200 µm and calcined at 700°C for 4 hours. Amorphous silica sourced from Rice Husk Ash (RHA) were obtained from Ndop, Northwest region of Cameroon and were milled to a particle size of 100 µm. An 8 M Sodium Hydroxide (NaOH) solution was prepared by dissolving sodium hydroxide pellets (98.7% VWR) in distilled water and allowed for approximately 24 hours to attain equilibrium after which it was mixed with sodium silicate (Na_2SiO_3) solution (molar $SiO_2/Na_2O \approx 3.5$, water content at 65 wt%) at a mass ratio of 2 Na_2SiO_3: 1NaOH and allowed for another 12 hours to stabilize [11]. Hydrogen Peroxide (H_2O_2) (10% w/v) and Aluminum powder (Al powder) were used as foaming agents. Three different surfactants: Triton H66 (anionic surfactant), Caflon and CG110 (nonionic) were used in selected matrices suitable for filtration. For trial runs of wastewater treatment, methylene blue (10% w/v) was used as a representative of wastewater (Table 1).

Characterization of raw materials

(Figure 1A and 1B) represent the infrared spectroscopy of clay rich laterite (both raw (R clay) and calcined (C clay)) and iron rich Laterite (both raw (Lb) and calcined (Lc)). The absorption band with a few intense peaks within the range of 3615 cm^{-1} and 3700 cm^{-1} which is later on shown to disappear after calcination in both materials indicating the elimination of this group. There is also an absorption band present at 1624 cm^{-1} to 1630 cm^{-1} represented in both raw and calcined forms of both materials [12]. These two band groups were ascribed to the stretching and bending vibration of hydroxyl group of either molecular water or absorbed water. The peaks present at about 948 cm^{-1} and 924 cm^{-1} in both figures were said to be represented by the asymmetric stretching vibration of Si-O-Si (Al). Finally the peak formed at 908 cm^{-1}, 796 cm^{-1} to 800 cm^{-1} could be attributed to Si-O stretching vibration characteristics but are also close to the values obtained by Moenka and Goodman, et al. for Al-O, Fe-O-Fe, Fe-O-Al, Fe-O-Si bonds. Finally, the band within the range of 625 cm^{-1} attributed to the bending vibration of Si-O.

Table 1: Chemical compositions of raw laterite and rice husk ash.

Oxides (wt. %)	Raw Laterite (Lat)	Rice Husk Ash (RHA)
Al_2O_3	17.93	52
SiO_2	25.3	87.01
P_2O_5	0.18	1.03
S_3O	0.05	0.18
K_2O	0.12	3.03
CaO	0.07	0.58
TiO_2	1.21	-
Fe_2O_3	41.23	0.5
Na_2O	-	-
MgO	-	-
MnO	-	-
Others	0.38	0.55
Loss On Ignition (LOI)	13.48	6.6
Al/Si	0.83	0.01

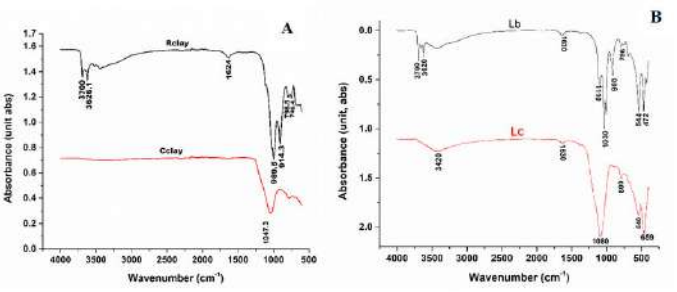

Figure 1: FT-IR spectrum of materials used: A) Clay material; B) Laterite material.

The nature of the crystalline phases present in the raw material was determined by XRD on the powder of both clay rich laterite (R clay) and iron rich laterite, (L) and are as presented in Figure 2. The X-ray pattern of uncalcined clay-rich laterite, Rclay (Figure 2a) and uncalcined iron-rich laterite, Lb (Figure 2b), shows the presence of the following crystalline phases: Quartz (SiO_2), Moganite (SiO_2); which is a polymorph of quartz, Hermatite (Fa_2O_3); which is the course of the reddish colour of the materials, traces of Anatas (TiO_2) and Cristobalite (SiO_2). Lb also showed the presence of Kaoline ($Al_2Si_2O_5(OH)_4$).

Upon the calcination of the iron-rich laterite, Lc (Figure 2b) also presented crystal phases like: Moganite, Hermatite and Quartz, with the intensification of the Quartz and Moganite peaks. Also it was observed that after calcination of the laterite soil, the kaoline crystal phase dissociated to form new crystal phases like: Tridymite (SiO_2), Berlinite ($AlPO_4$), Feldspare ($NaAlSi_3O_8$) and small amounts of Cuprite (Cu_2O) around same regions where Kaolin were found in the uncalcined material [13].

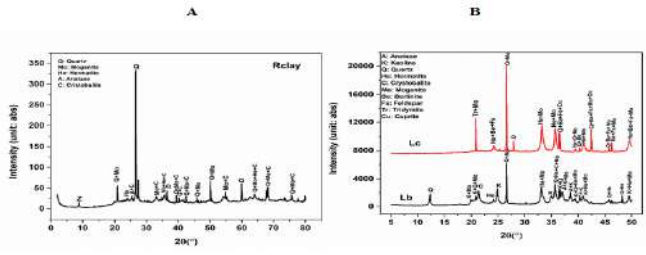

Figure 2: X-ray pattern of: A) Clay; B) Laterite.

Besides these crystalline phases, the X-ray pattern of the calcined laterite (Lc) indicates a broad hump structure between 20°C and 35°C (20°C) centred at around 25°C (20°C). The presence of this halo diffraction implies the formation of amorphous phases in Lc due to calcination of laterite.

Preparation of filtration matrices

For the preparation of the matrices, the aluminosilicate source (either calcined clay rich laterite or iron rich laterite) were varied

in mass with RHA to sum a total mass of 100 g. The solid components (Aluminosilicate and RHA) were then mixed with the alkaline activation solution at a solid, liquid (S/L) mass ratio of 1.4 using a multispeed mixer for about 5 minutes to obtain a fresh paste. The direct foaming method Bai, et al. was applied in which either Al powder or H_2O_2 at different quantities were added to the fresh paste and mixed for another 3 minutes [14-17]. The paste was then poured into cylindrical molds of dimension 9.84 cm diameter and 1.5 cm thickness and oven cured at 60°C for 2 hours. The quantities of foaming agent used were 5 mL, 7 mL and 9 mL of hydrogen peroxide or 0.02 g, 0.04 g, 0.06 g and 0.08 g of Al powder. After curing, the geopolymer foams were allowed for 28 days in an air tight plastic bag to minimize efflorescence, before any characterizations were done.

Characterization of filter matrices

Characterization of physical characteristics of foams: The apparent Porosity (P), Bulk density (B) and water Absorption (A) of the samples were studied by means of Archimedes method. Samples were oven dried at 150°C for approximately 24 hours and their masses obtained as "D". The dried samples were then submerged in distilled water for another 24 hours after which the saturated Mass (M) and suspended mass under water (S) were obtained and the interested characteristics were obtained using the following equations;

$$V = M - S \quad \text{Eq1}$$

$$P = \frac{[M-D]}{V} * 100 \quad \text{Eq2}$$

$$B = {}^{D}/_{V} \quad \text{Eq3}$$

$$A = \frac{[M-D]}{D} * 100 \quad \text{Eq4}$$

These properties enabled the selection of matrices suitable for filtration for which only samples which had a consistent apparent porosity and water absorption of 25% and above were selected.

Characterization of permeability: To measure the permeability of the selected materials, their surfaces were polish with abrasive paper at both ends to expose the pores and to make them have a uniform thickness of 1.0 cm. each matric was placed in a 30 cm long column with a head space of 25 cm, the edges sealed with silica gel seal and water poured to the head space to fill it [18]. The constant head water permeability coefficient (K) was then calculated using equation 5. where p is the water head (cm), A, the sample area (cm^3), h, the sample height (cm), Q, the flow rater of water (cm^3/s), η20, water viscosity at 20°C and ηT, water viscosity at the measured temperature.

$$K = \frac{\eta_t}{\eta_{20}} * \frac{Q*h}{A*p} \quad \text{Eq5}$$

Characterization of composition and structure: To characterize the morphology of the geopolymer foam, a high resolution scanning electron microscope was used. To identify the different compounds formed during geopolymerization and function groups present in the foams, infrared spectroscopy (FTIR) was done. The crystalline phase of the raw materials and geopolymer foams were evaluated by means of x-ray diffractometry.

Optimization of permeability of porous geopolymer: To increase pore uniformity and connectivity of the selected foams, one of the samples was selected (C20R7H) and the formulation used with either of the three surfactants (triton H66, caflon and CG110) at volumes 0.2 mL, 0.4 mL, 0.7 mL and 1 mL. The formulations were done after which their permeability were evaluated as earlier mentioned to obtain the most suitable surfactant and the appropriate quantity to use to obtain the best permeability [19].

The selected surfactant and appropriate quantity to be used were then used to reproduce the selected filtration matrices. Their physical properties and permeability were evaluated to determine the effect of the surfactant on the matrices.

Dye removal trail: A filter, each from both base materials (laterite and clay) was chosen from the selected matrices and casted into a PVC column as earlier mentioned in the permeability test. 1.5 L of methylene blue (10% v/w) was then poured into the column and filtration done under atmospheric conditions (atmospheric pressure). Evidence of methylene blue removal from water was verified using the Ultraviolet-visible light (UV-Vis) spectroscopy (Shimadzu UV-1800) to quantify MB in the experiment at a wavelength of 664 nm by using quartz cuvettes. Filtrates were collected every 30 minutes and analyzed. The amount of MB removed was obtained as expressed in equation 6.

$$MB\ removed\ [\%] = \left[\frac{(C_0 - C_t)}{C_0}\right] * 100 \quad \text{Eq6}$$

Where,

C_0 is the initial concentration of MB.

C_t is the concentration of MB at time t after filtration.

For evidence or to verify if the filters contributed in the treatment by removal of dye, an infrared spectroscopic analyses was done on the filters used before and after dye treatment to evaluate the formation or presence of new functional groups in the filter.

RESULTS AND DISCUSSION

Effects of rice husk ash on the physical properties of geopolymer foams

The effect of RHA on the physical properties (apparent porosity, bulk density and water absorption) of both clay-rich laterite based and iron-rich laterite based porous materials using either Hydrogen Peroxide (H_2O_2) or Al powder as foaming agent is as presented in Figures 1-3.

Increasing the RHA (amorphous silica) content from 0% to 50% solid mass showed a scatter of values for both clay-rich laterite based and iron-rich laterite based porous geopolymer using either H_2O_2 or Al powder as foaming agent. The apparent porosity fluctuated to a maximum at 30%, 20% and 40% RHA for clay-rich laterite based porous geopolymer (Figures 3A and

3B), 0%, 10% and 40% RHA for iron-rich laterite bases geopolymer foams (Figure 3C) using 5 mL, 7 mL and 9/10 mL of hydrogen peroxide respectively; 5%, 40% 50% and 20% RHA for clay-rich laterite based (Figure 3B), 40%, 40% and 10% RHA content for iron-rich laterite based geopolymer foams (Figure 3D) using 0.02 g, 0.04 g, 0.06 g and 0.08 g of Al powder respectively as foaming agent. From the maximum, they only reduced from there on for each concentration of either of the foaming, most of the highest porosity were only obtained after a reasonable quantity of RHA was added to the material [20]. This could be affiliated to the fact that, the presence of RHA (amorphous silica) in the matrix arranges the pores and created some degree of pore interconnectivity. This was an exception when 5 mL of H_2O_2 was used, as the apparent porosity was observed to be almost steady (Figure 3A) or reduced with increase in RHA content (Figure 3C). The reason for this could have been that, the addition of amorphous silica to geopolymer will led to an increase in the Si/Al ratio of the matrix, which favors the formation of a homogenous microstructure with compactness. Also, given that H_2O_2 is a mild foaming agent, low concentrations will not be able to create a remarkable foaming impact as the RHA content increases. Further analysis indicated that increase in H_2O_2 content lead to increase in apparent porosity which confirms the earlier made observation [21].

This observations made were not same for the porosity of geopolymer with aluminium powder as foaming agent. For the calcined clay-rich laterite porous geopolymer, it was observed that the best porosity was obtained at 0.06 g Al powder and 50% RHA (Figure 3B). Low concentration of Al powder (0.02 g), gave optimum porosity at low RHA content (0.02 g Al powder and 5% RHA content) while subsequent concentrations gave optimum porosity at higher RHA content (20%-50% RHA). For iron-rich laterite based porous geopolymer, it was observed that best porosity where obtained at low concentrations of Al powder (0.04 g) and at high RHA content (40%) while at high Al powder concentration (0.08 g), optimum porosity was formed at low RHA content (10% RHA). Porous geopolymer produced from both materials using Al powder did not increase with increase in amount of Al powder as the %RHA increases as predicted by Novais, et al., Ogundiran, et al., Eliche-Quesada, et al. From these findings, it was obvious that the %RHA (amorphous silica) in the matric had some role to play with respect to increasing the Si/Al or Al/Fe ratio leading to compactness of matric hence, the apparent porosity as predicted by Kamseu, et al., but the use of Al powder as porous agent might have some effect on the chemical composition of the material during the formation of pores in accordance to equations (1,2,3) as noted by Mohammadian and Al Bakri, et al.

$$2Al + 6H_2O \rightarrow 2Al(OH)_2 + 3H_2 \quad \text{.....Eq7}$$

$$2Al + 3H_2O \rightarrow Al_2O_3 + 3H_2 \quad \text{.....Eq8}$$

$$2Al + 6H_2O + 2NaOH \rightarrow 2Na[Al(OH)_4] + 3H_2 \quad \text{.....Eq9}$$

From here, it can be said that the addition of Al powder might have some degree of influence on the aluminum composition of the material hence influencing the Si/Al ratio of the matric which will affect the degree of polymerization and hence the apparent porosity in an unpredictable manner.

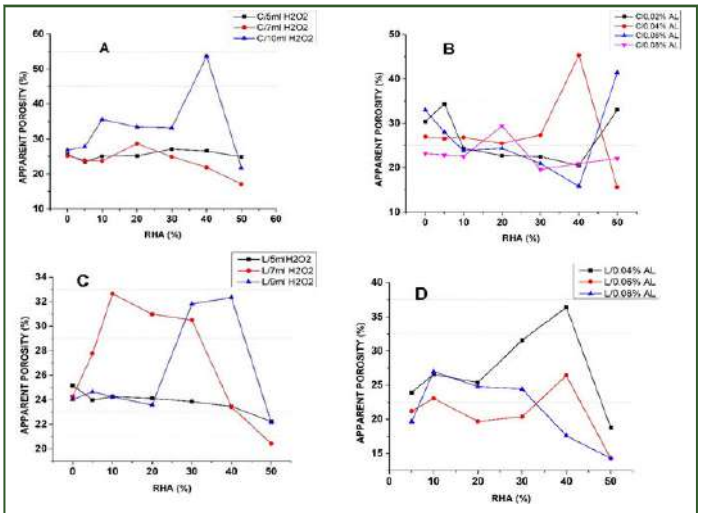

Figure 3: Effect of RHA content on the apparent porosity of porous geopolymers from: A) Clay-rich laterite based and H_2O_2; B) Clay-rich laterite based using Al powder; C) Iron-rich laterite based using H_2O_2; D) Iron-rich Laterite based using Al powder foaming agent.

Evaluating of the bulk density of the porous geopolymer from both based materials indicated a scatter of value as the RHA content increased for each concentration of foaming agent. The

bulk density of porous geopolymer produced using H_2O_2 as foaming agent (Figures 4A and 4B) were observed to follow an almost opposite trend from the apparent porosity as porosity increased leading to bulk density decrease. Similar results were obtained by Eliche-Quesada, et al., and Novails, et al. which stipulates that an increase in porosity leads to reduction in bulk density. On the other hand, porous materials made from both materials using aluminum powder as foaming agent (Figures 4C and 4D) present an undulating though almost similar in trend to that of their respective apparent porosity for each concentration of Al powder and varied with RHA content. Since the bulk density of a material is always related to the microstructure of the material and the presence of amorphous silica favors pore connectivity and polycondensation as stipulated by Rodrigue, et al., this could be related to the degree of pore connectivity caused by RHA. Hence pore connectivity was more favored in geopolymer foams produced using H_2O_2 as foaming agent than Al powder. It was also observed from the results that most of the densest matrices were obtained when RHA was added especially between 20%-40% RHA composition which was attributed to the reason that amorphous silica source increases the amount fraction of amorphous phase and also improves the chemical bonds, Si-O-Fe, Si-O-Al and the formation of ferrosialate as well as iron silicate, which allowed dense matrix and re-equilibrates the Si/Fe, Si/Al and Al/Fe ratios during the alkaline activation as stipulated by Rodrigue, et al. Hence these results were seen to be a confirmation of those of the apparent porosity.

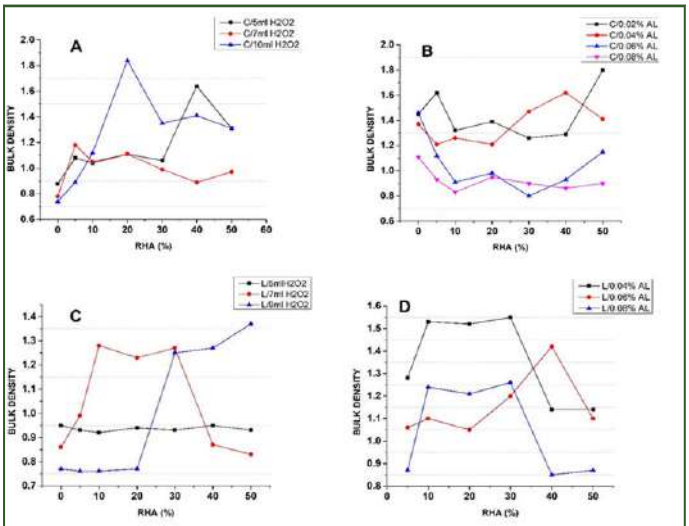

Figure 4: Effect of RHA content on the bulk density of porous geopolymers from: A) Clay-rich laterite based and H_2O_2; B) Clay-rich laterite based and Al powder; C) Iron-rich laterite based and H_2O_2; D) Iron-rich Laterite based and Al powder foaming agent.

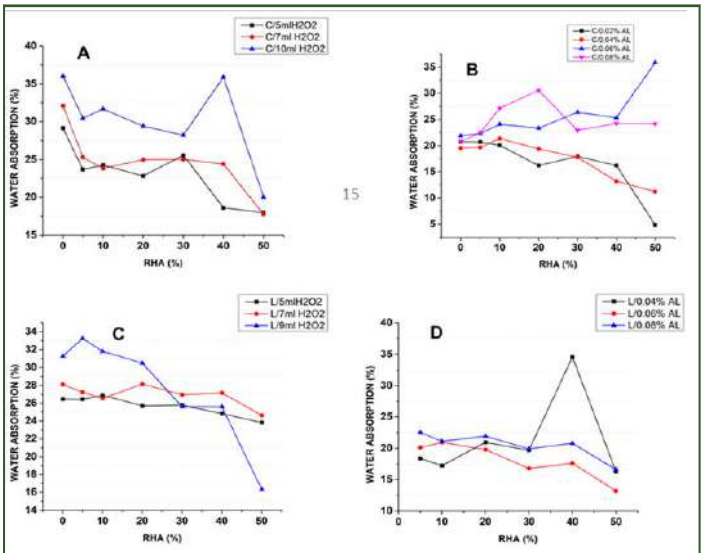

Figure 5: Effect of RHA content on the water absorption of porous geopolymers from: A) Clay-rich laterite based and H_2O_2; B) Clay-rich laterite based and Al powder; C) Iron-rich laterite based and H_2O_2; D) Iron-rich Laterite based and Al powder foaming agent.

The water absorption of the either clay-rich laterite based or iron-rich laterite based porous geopolymer is presented in Figure 5. In general, there was observed to be a similar trend as reported in Figure 1 and 2. Producing porous geopolymer using H_2O_2 as foaming agent required less than or equal to 15% RHA content in both base material to attain an optimum water absorption. Subsequent addition of RHA will only lead to a reduction in the water absorption nor matter the amount of H_2O_2 being used. This decrease in water absorption with increase in %RHA content (increase in amorphous silica composition) in the case of using H_2O_2 as foaming agent could be affiliated to the fact that, increase in RHA favors the connectivity and polycondensation of raw materials, improves the cohesion between particles and leads to smaller pores occurred into the matrix network as stipulated by Rodrigue, et al. Hence making the pores to be inaccessible by water as water resides in pores. The use of Al powder as porous agent in both base materials showed some interesting results in that they required higher amount of RHA to reach a maximum absorption than those producing using H_2O_2 as foaming agent. It was noted that for the clay-rich laterite based porous geopolymer (Figure 5B), increasing the amount of Al powder led to an increase in the quantity of RHA needed to reach maximum absorption. Meanwhile for the iron-rich laterite based porous material (Figure 5D), increasing the amount of Al powder required lesser amount of RHA. From these findings it could be said that even though the presence of RHA affects the water absorption as stipulated by Rodrigue, et al. it might also be that the addition of Al powder might have some influence on the chemical composition of the gel in that, during its reaction to produce pores, aluminum oxides and hydroxides are formed as stipulated by Mohammadian, et al. Al Bakri, et al. which may affect the Si/Al or Al/Fe ratio of the gel which are factors that affect the degree of polycondensation during geopolymerization hence impacting the porosity hence water absorption.

Effects of foaming agent content on the physical properties of porous geopolymer

The effects of forming agent quantity and type on the apparent porosity, bulk density and water absorption of porous geopolymer is as presented in Figures 4-6 respectively.

The introduction of Hydrogen Peroxide (H_2O_2) as foaming agent into both clay-rich laterite and iron-rich laterite based porous materials (Figures 6A and 6B) showed mostly an increase in

apparent porosity with the increase in H_2O_2 quantity (5 mL-10 mL) for most %RHA content in the matric except in the clay-rich laterite based porous geopolymer for which at high %RHA (≥ 30%) composition. The porosity was mostly seen to decrease with increasing quantity of H_2O_2. This suggests that using hydrogen peroxide as foaming agent will produce good pores but it will depend on the silica content of the geopolymer paste. When Al powder was used as foaming agent (Figures 6C and 6D), it was observed that increasing in the amount of Al powder led to mostly a decrease in the apparent porosity for most of the %RHA content. This could be attributed to the fact that when the amount of Al powder increases, there is high speed of the reaction and the porous structure produced by the foaming agents is stable only for a short time and then falls after a while (before the bonding process-geopolymerization) as outlined by Lach, et al. Also, it was seen that the pores obtained from hydrogen peroxide were more uniformed and mostly in the range of micro to macro pores while those obtained from Al powder were not uniform with range within macro to mega pores and the presence of holes. This may be due to the well-controllable decomposition of hydrogen peroxide and the possibility of homogeneously distributing the foaming agent within the geopolymer gel as suggested by Bai and Colombo, compared to Al powder for which the redox reactions are intense due to the high alkalinity of the system, hence, making it difficult to control the generated cell size and total porosity.

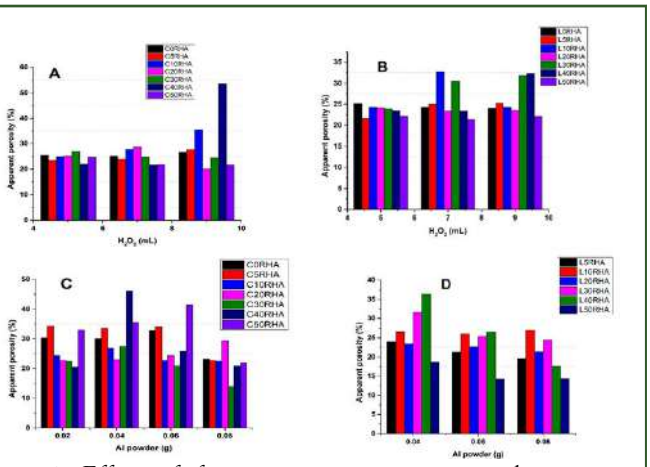

Figure 6: Effect of foaming agent content on the apparent porosity of porous geopolymers from: A) Clay-rich laterite and H_2O_2; B) Iron-rich laterite and H_2O_2; C) Clay-rich laterite and Al powder; D) Iron-rich Laterite and Al powder foaming agent.

Computation of the bulk density of the porous geopolymer obtained from both base materials using H_2O_2 as foaming agent (Figures 7A and 7B) showed that, the bulk density mostly decreased with increase in the amount of H_2O_2 content for most of the matrices with low %RHA content. But at higher %RHA content (≥ 30%), increase in H_2O_2 content only resolved to an increase in the bulk density. Here, it was clear that the increase in the H_2O_2 content of the paste led to the introduction of more gas in the paste during its decomposition hence increasing the porosity hence decrease in the bulk density of the matric. But this trend is obstructed when the %RHA content becomes high, leading to the increase in bulk density of the matrix. This will imply that, high Si content in geopolymer will destabilize the pore foaming process. Thus, the porous structure produced by foaming agents is stable only for a short time and then falls after a time, hence confirming the results of the apparent porosity.

The bulk density of the porous geopolymer produced with Al powder as foaming agent (Figure 7C and 7D) showed mostly a decrease in bulk density as the amount of Al powder increased for each %RHA content. This was a confirmation to the results obtained for the apparent porosity as the bulk density increase when apparent porosity decreases. This could be affiliated to the reason that with the difficulty involved in controlling the generated cell size and porosity during foaming, the cell form by this route are typically closed as stipulated by Bai, et al.

Computation of bulk density was observed to range from 0.74 g/cm^3 to 1.84 g/cm^3 and 0.76 g/cm^3 to 1.37 g/cm^3 for clay based and laterite based porous geopolymer respectively using H_2O_2 as foaming agent while using Al powder as foaming agent had apparent porosity within the range of 0.79 g/mm^3 to 10.79 g/mm^3 and 0.87 g/mm^3 to 1.55 g/cm^3 for clay base and laterite base porous geopolymers respectively.

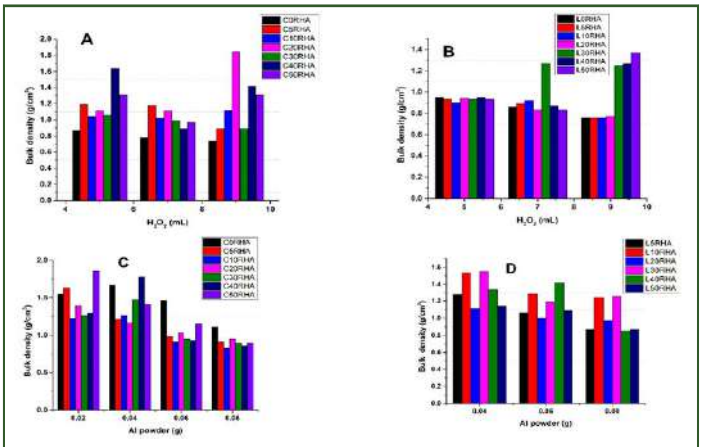

Figure 7: Effect of foaming agent content on the bulk density of porous geopolymers from: A) Clay-rich laterite and H_2O_2; B) Iron-rich laterite and H_2O_2; C) Clay-rich laterite and Al powder; D) Iron-rich Laterite and Al powder foaming agent.

The results of the influence of foaming agent on the water absorption from the porous geopolymer are presented in Figure 6. Computation of the water absorption from both base materials using both foaming agents mostly indicated an increase in the water absorption with increase in the foaming agent content for each %RHA content except in some geopolymer foams labelled C20RHA, L40RHA, L50RHA with H_2O_2 as foaming agent and C0RHA, C30RHA, C50RHA with Al powder as foaming agent, where the water absorption had scattered values but the trend showed an increase then decrease in water absorption with increase in amount of foaming agent or L40RHA using Al powder as foaming agent, in which there was observed to be a decrease in water absorption values with the increase in the amount of foaming agent.

It was therefore evident that an increase in foaming agent content will lead to the formation of more pores which will lead to increase in water absorption because there is availability of more empty space for water to reside within the porous geopolymer. Though porous geopolymers produced with Al powder were considered to have closed pores but they showed a high water absorption value which will only mean that the presence of large pores and holes present in the matrix influenced the water absorption of the matrices.

Stability in water of porous geopolymer

The water stability of the porous geopolymer were obtained by measuring the mass of each matrix left in water after 14 days and 28 days and the percentage mass difference were computed from 1 day water absorption to determine if the material degraded or were stable with time. Results for water stability test is reported in for clay-rich laterite based and iron-rich laterite based porous geopolymer using either of the porous agents. Observations made from stability test indicated that though there were instances where the matrices degraded over time, in most cases, increase in the foaming agent content leads to increase in stability of the matrix. This stability was also seen to depend on the %RHA content in the matric as stable matrices were

observed to be mostly between 0% and 30% RHA and matrices with RHA content of 50% were mostly found to be unstable as their masses degraded with time which could be attributed to the fact that when the SiO_2 is high in geopolymer gel it makes it to have a plastic behavior which would imply that geopolymers made with high amounts of RHA are not suitable as structural materials as outlined by Fletcher et al. Further observations indicated that matrices made using hydrogen peroxide as foaming gent were more stable than those made with Al powder.

In this work, the matrices suitable for application in wastewater filtration were selected by means of comparison of results of apparent porosity and water absorption then evaluating their stability. Only matrices with an apparent porosity and water absorption ≥ 25% with consistent selections we chosen and their water stability evaluated for validation. Give the matrices or samples that were selected for further application in filtration. Matrices selected indicated that they were mostly those produced using hydrogen peroxide as foaming agent fell
within the given criterial of selection. This indicated that H_2O_2 is the preferable foaming agent than Al powder probably because it foaming process is gentle and stable producing uniform size and distribution of pores hence suitable for filtration.

Phase evolution of porous geopolymer

The infrared spectra of clay-rich laterite based and iron-rich laterite based porous geopolymer produced using both Al powder and hydrogen peroxide as foaming agent are presented in (Figures 8A and 8B) respectively. From (Figure 8A and 8B), the broad band at 3000 cm^{-1}-3600 cm^{-1} and at 1635 cm^{-1}-1650 cm^{-1} correspond to the stretching and deformation modes of H-O-H and O-H of water molecules. These bands were observed to be absent on the spectra of C20R8Al but instead a strong band aroused at 3638 cm^{-1} which could be attributed to the phase symmetric stretching of OH water coordinated to either Al or Mg as reported by Balan, et al. This confirms that the addition of Al powder as foaming agent has an impact on the chemical structure of some geopolymer gel. The strongest band in the region of 970 cm^{-1}-1300 cm^{-1} with maximum at around 980 cm^{-1} could be attributed to the symmetric stretching vibration of Si-O-T (T=Al, Fe or Si) and these peaks have been described as the characteristic peak of geopolymer binder structure as outlined by Rodrigue, et al. But this peak is seen to shift to a higher wave number of 1394 cm^{-1} in in C20R8Al with reasons being that this stretching mode are sensitive to the Si/Al ratio and may shift from the usual wave number with increase in number of tetrahedral Al atom as stipulated by Davidovits, et al. Those around 1380 cm^{-1} -1390 cm^{-1} are linked to stretching of C-O bonds in all spectra due to the formation of sodium/iron carbonate due to reaction of residual or unreacted alkali metal with CO_2 of the atmosphere as noted by Rodrique, et al.

From the data obtained for both clay based and laterite based porous material, it exhibited other bands at 872 cm^{-1}, 786 cm^{-1}, 712 cm^{-1} and 629 cm^{-1} (Figure 8A) and 786 cm^{-1} (Figure 8B) which can be assigned to different tetrahedral framework atoms vibrations in the silicate structure. The absorption band at 872 cm^{-1} (Figure 8A) could be attributed to the AlFeOH bending as stipulated by Diana, et al., band at 771 cm^{-1} to 788 cm^{-1} (Figure 8a) and 786 cm^{-1} (Figure 8b) were ascribed to Si-O-Al bonds symmetric stretching in both clay based and laterite based porous materials respectively Yunsheng, et al.. The small absorption band at 629 cm^{-1} were attributed to the Si-O-Al (IV) stretching of the tetrahedral network which ae close to the value obtained by Tchakoute, et al.

The strong peak at about 3638 cm^{-1} which was attributed to the stretching of OH of water molecule coordinated to Al portrayed by geopolymer foam in which Al powder was used as foaming agent indicated that the use of this foaming agent might play on the wastewater characteristics during treatment as some of the metal composition might leach into the solution as it passes through the matric.

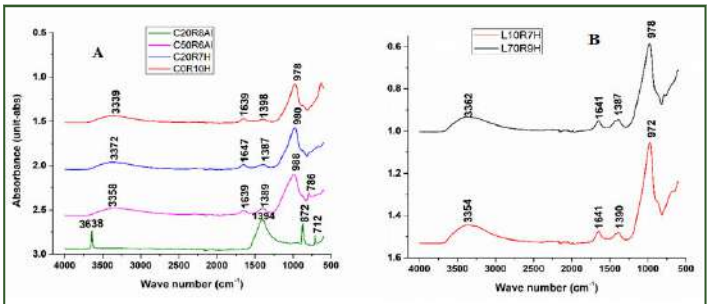

Figure 8: FTIR of porous geopolymer. A) Clay based porous geopolymer; B) Laterite based porous geopolymer.

The X-ray patterns of selected geopolymer foams produced from either calcined clay-rich laterite (C0RHA5H; C20RHA5H; C20RHA8A) or calcined iron-rich laterite (L0RHA7H; L20RHA7H; L30RHA8A) are presented in (Figures 9A and 9B) respectively. The X-ray patterns of C0RHA5H and L0RHA7H exhibits humbs throughout the diffractogram and are mostly dominated by mineral phase for both clay based and laterite based geopolymer foams, followed by traces of moganite (SiO_2) and hematite (Fe_2O_3): in the laterite based geopolymer foam. These phases are also observed in the calcined material (Figure 9), which will suggest that they were not involved in the geopolymerization reaction. These humbs (amorphous content) are observed to increase with Rice Husk Ash (RHA) content moving from C0RHA5H to C20RHA5H and L0RHA7H to L20RHA7H in both clay-rich laterite based and iron-rich laterite based geopolymer foams respectively. This observation was also made by Kamsue, et al., who worked on the increase of RHA content on laterite based composite. It was observed that the increase in RHA content also lead to the disappearance of the moganite and hematite phase while the iron-rich laterite based geopolymer foam exhibited traces of cristobalite SiO_2 and Anatase TiO_2 phases when the RHA content was increased. The pattern also exhibited a dominant phase of quartz.

Substitution of hydrogen peroxide with aluminum powder as foaming agent in C20RHA8A and L30RHA8A samples. The diffractograms indicated that the geopolymer foams are more crystalline in comparison to when hydrogen peroxide was used alone as foaming agent. The X-ray pattern of these two geopolymer foamsexhibited a typical halo structure between 20° and 35° (2θ) and centered around 24° (2θ) in both diffractograms. It was observed that the intensity of the

quartz phase decreases and new phases formed including kalsilite ($KAlSiO_4$), sanidine $KAlSi_3O_8$, cristobalite (SiO_2) in clay-rich laterite bases geopolymer foams and magnetite Fe_3O_4, tridymite SiO_2, in iron-rich laterite based geopolymer foam. This confirms that the use of Al powder as foaming agent plays an impact in the composition of geopolymers forms, introducing new phases making it more crystalline which may be good in increasing its strength but might not be suitable in wastewater treatment.

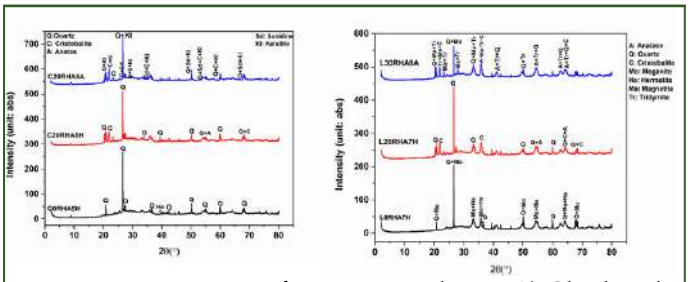

Figure 9: X-ray pattern of porous geopolymer. A) Clay based; B) Laterite based.

Microstructure of porous geopolymer

The micrograph of selected clay based and laterite based porous geopolymer produced from either H_2O_2 or Al powder as foaming agent cured at 65°C for 2 hours are as shown in Figure 10. The images were analyzed at different magnification (34 x, 70 x, 80 x, 140 x, 160 x, 280 x and 300 x) in order to clearly identify the morphological nature and the pores of the porous geopolymer. All specimens showed the presence of pores of different sizes which are mostly closed and depend on the concentration of foaming agent and RHA content. Increasing the amount of foaming agent content (Figure 10) leads to the increase in the pore size and mostly large pores were created. Introduction of amorphous silica (RHA) in an appropriate quantity will lead to organization of the pores hence creating almost uniformly distributed pores (sample L5RHA9H) as compared to the geopolymer without RHA (C0RHA7H and C0RHA10H). Increasing the amount of RHA content in the porous geopolymer samples was observed that though the pores were arranged, the matrix became more compact with mostly dense structure being observed (L30RHA9H). The use of Al powder as foaming agent indicated the formation of different classes of pores which are mostly mega pores on the micrograph (C20RHA8A) as of compared to when H_2O_2 as foaming agent.

In the micrograph, sodium carbonate salt deposits from efflorescence can also be observed on the surfaces of the materials and these are in porous geopolymer produced using H_2O_2 as foaming agent than aluminum powder.

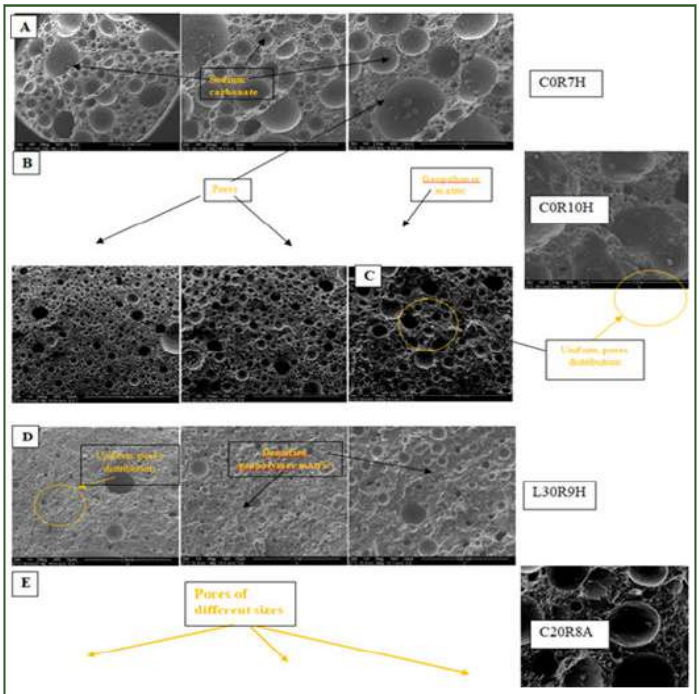

Figure 10: SEM micrograph of clay based and laterite based porous geopolymer showing the evolution of the microstructure as function of foaming a get content, RHA content and foaming agent type.

Water permeability of porous geopolymers

It is important for a filter need to have adequate water permeability in order to ensure flow of water through the filter so it can be applicable in wastewater treatment. This water permeability is said to mostly depend on the pore size and shape as well as their connectivity as outlined by Youmoue, et al. In this study, the water permeability was evaluated with respect to the water flow rate of the selected porous materials. It was observed that water got through to from one end to the other of the material but they was no flow out recorded in terms of mL of water through. The only explanation that could be affiliated to this observation was that though the materials were highly porous, the pores had very little connectivity hence hindering water from flowing through appreciably.

For these materials to be applicable in wastewater filtration, there is the need to stabilize the pores which will help to increase pore connectivity hence making flow of water appreciable. Literature has it that the addition of surfactant to geopolymer will help stabilize the pores and enhance connectivity. In this study three surfactants where used: Triton H_{66}; caflon; CG110.

Optimization of the permeability of selected porous materials

Effect of surfactant on the porosity and permeability of porous geopolymer: In this study, the formulation of one of the selected specimen (C20RHA7H) was chosen and formulation tried with either of the three surfactants at different volumes. The flow rate of the matrices obtained was evaluated to

determine the best surfactant to be used and the appropriate quantity to be used. Table 2 present the results obtained.

Table 2: Evaluation of the flow rate of matrices produced from different surfactants.

Sample formulation	Triton H66 mL				Caflon mL	CG110						
Quantity	0.2	0.4	0.7	1	0.2	0.4	0.7	1	0.2	0.4	0.7	1
Flow rate mL/30	15	24	9	7	3	1	1	1	2	2	1	1

From the flow rate results obtained, it was observed that the use of triton H_{66} as surfactant at 0.4 mL gave the best flow rate, so it was used to optimize the permeability of the selected filters.

Influence of surfactant on the physical properties of porous geopolymer: The influences of the surfactant on the physical properties (apparent porosity, bulk density and water absorption) of the porous geopolymer were evaluated and are as presented in Figure 11. Observations made were that, the addition of the surfactant to the selected geopolymer matrices increased the apparent porosity prominent consequently leading to reduction in their respective bulk density and also an increase in their water absorptions due to availability, accessibility and increase in the number of pores, reason being that combined addition of foaming agent and surfactant results in the formation of open pores. This is because addition of a surfactant led to the stabilization of the gas-liquid interface by hindering bubble coalescence, continuous Ostwald ripening or spontaneous drainage. Further analysis of results indicated that these changes observed were not really remarkable in matrices without RHA, like L0RHA5H, C0RHA7H and C0RHA5H. When the foaming agent content was increased in same condition, like in the case of C0RHA5H to C0RHA7H, there was also a recognizable change in the resulting measured properties hence confirming the findings as earlier stipulate that presence of RHA (amorphous silica) will help organize the pores and create some degree of pore connectivity and increase in the amount of foaming agent will lead to increase in the porosity subsequently affecting other properties like bulk density and water absorption.

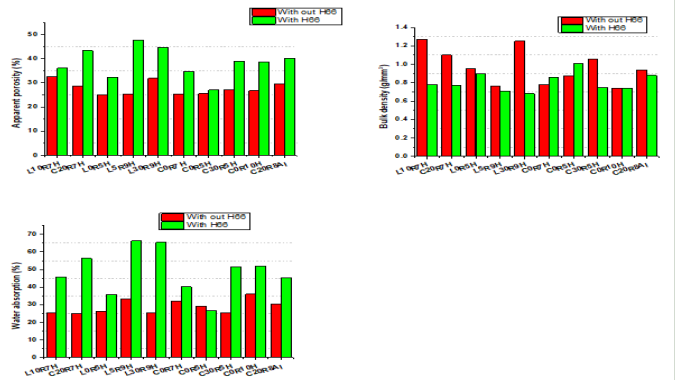

Figure 11: Influence of the addition of Triton H66 on the physical properties of selected porous geopolymers. A) Apparent porosity of porous geopolymers; B) Bulk density of the porous geopolymers; C) Water absorption of the porous geopolymers.

The augmentation of the physical properties (apparent porosity, bulk density and water absorption) of the geopolymer foams when surfactant was added as of compared to the geopolymer foams without surfactant, was a clear evidence that the introduction of surfactant increased pore connectivity. The visual confirmation is as represented in the microstructure of both samples in Figure 12 which shows the difference in pore structures in both cases.

Figure 12: Pictorial presentation of the porous geopolymer. A) Initial porous geopolymer; B) Optimised porous geopolymers.

Evaluating the water flow rate of the selected porous geopolymer

The water flow rate of the selected porous geopolymer were obtained in accordance to the filtration setup, to evaluate the water permeability of the geopolymer matrices. Effluents from the matrices were collected after every 30 minutes. The results are as presented in Table 3. This results enabled further elimination of matrices not suitable for wastewater treatment, as materials for efficient filtration are not supposed to have a high water flow rate in order to be highly interactive with matrices so as to have an appreciable absorption and adsorption of pollutants.

Table 3: Water flow rate evaluation of selected porous geopolymers.

Name	Volume of water collected per time		
	30 mins	**60 mins**	**90 mins**
L30R9H	105 mL	94 mL	80 mL
L5R9H	105 mL	83 mL	91 mL
L10R7H	30 mL	27 mL	28 mL
L0R5H	250 mL	190 mL	210 mL
C50R6A	0	0	1 mL
C20R8A	1162 mL	893 mL	910 mL
C0R10H	540 mL	490 mL	503 mL
C30R5H	125 mL	109 mL	111 mL
C0R5H	340 mL	321 mL	307 mL

Eliminated due to high flow rate: From the flow rate measurements, the porous materials could be classified according to their porosity, ranging from very porous to slightly porous. This classification can enable them to be applicable at various stages of the wastewater treatment system (that is: Preliminary, primary, secondary or tertiary stages of treatment) Table 4 resent this classification of porosity with respect to their flow rate or water permeability.

Table 4: Porosity Classification of selected geopolymer foams with respect to water permeability.

Very porous	Averagely porous	Porous	Slightly porous
C50R6A	L30R9H	L10R7H	C50R6A
C0R10H	C30R5H		
C0R5H	L5R9H		
	L0R5H		

Wastewater (methylene blue) treatment trial: Two samples; one from each base material, were selected and applied in the filtration setup as earlier presented in Figure 13. The results from the treatment of wastewater (10% w/v methylene blue) is presented in Figure 14. Filtration efficiency revealed by the filters from the removal of methylene blue was 100% for the first 5 hours-6 hours with effluent been collected and analyzed every 30 minutes. Close to the 7th hour of treatment, the methylene blue removal efficiency started dropping to a value of 97% after 8 hours. Matrices containing higher than 20% rice husk ash content showed an even lower efficiency of 95% close to the end. The efficiency depended on RHA content, which is a factor that influences pore connectivity.

Though the presence of pores are said to be a principle requirement for increased adsorption of ions and minerals (pollutants) as postulated by Tee, et al. it was observed that increased RHA content lead to increased pore connectivity which reduced the treatment efficient, as not all the dye in water were removed by the porous geopolymer in the case were the RHA content was high. This will mean these porous materials exhibited a promising outcome to remove dye from water using different mechanisms of filtration (adsorption, absorption and course blockage), hence can be applied for the practical treatment of wastewater.

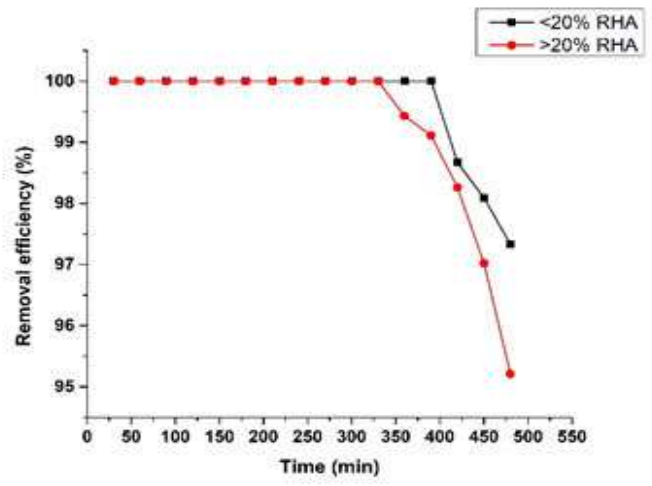

Figure 13: Methylene blue removal efficiency as a function of time.

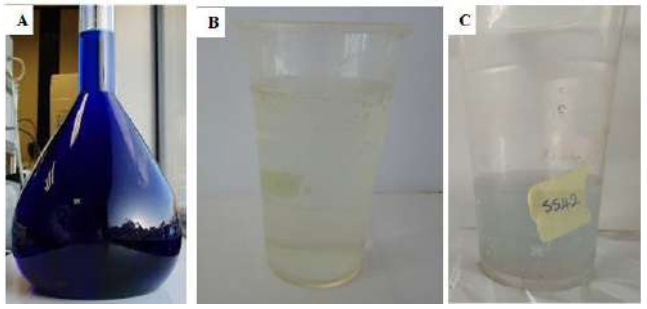

Figure 14: A) Methylene blue influent; B) Effluent from filter containing <20% RHA content; C) Effluent from filter containing >20% RHA content.

To confirm the porous geopolymers' potential to treat wastewater, powdered samples were collected from the each of the membranes involved in wastewater treatment before and after wastewater treatment and an infrared spectroscopic analysis (FTIR) done. The two spectrographs from each sample were analysed by superimposing them to evaluate the formation of new peaks (new functions groups). Results obtained from the FTIR analysis is as presented in (Figures 15A and 15B). apart from the conventional peaks found in geopolymers, including the broad band at around 3370 cm^{-1}-3390 cm^{-1} and that at around 1640 cm^{-1} affiliated to the stretching and bending vibration of hydroxyl group of water molecule, band within the range of 965 cm^{-1}-980 cm^{-1} attributed to Si-O-T (T=Al, Fe or Si), peak at around 1380 cm^{-1}-1390 cm^{-1} ascribed to the stretching of C-O bonds and those at 678 cm^{-1}-688 cm^{-1} and 524 cm^{-1}-534 cm^{-1} attributed to the vibrations of Al-O-Si and Si-O-Si respectively, there is the formation of a new peak in the used geopolymer foams (C0RHA10H and L5RHA9H) at around 395 cm^{-1}. This peak clearly indicates the vibration of a new function group in the geopolymer foam which might have been initiated by the C-N-C vibration in MB as outlined by Raiyaan, et al.

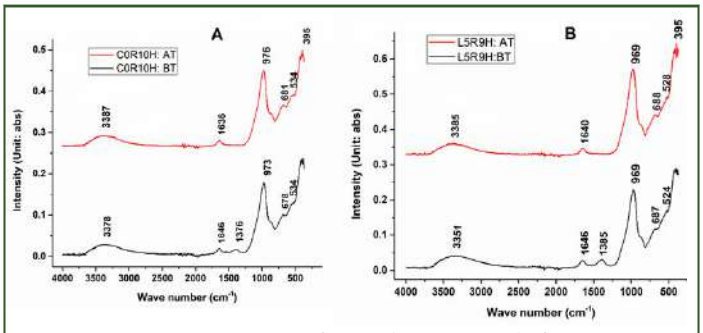

Figure 15: FTIR spectra of membranes used for wastewater treatment before and after treatment; A) Clay based; B) Laterite based porous geopolymer.

CONCLUSION

Porous geopolymer membranes were prepared using 2 different aluminosilicate sources (clay-rich laterite and iron-rich laterite), rice husk ash (amorphous silica), two different foaming agents (H_2O_2 and Al powder) and three different surfactants (Triton H66, Caflon and CG110). The addition of either of the foaming agent lead to the formation of pores as identified with the scanning electron microscopic analysis. Introduction of rice husk ash of up to 20% solid content in the matric improved the physical properties (porosity, bulk density and water absorption) and the pore structure of the porous geopolymer. Selection of matrices suitable for filtration from physical properties indicates that matrices prepared with hydrogen peroxide were more feasible in wastewater treatment than those produced with aluminum powder. This was confirm with the infrared spectroscopic analysis and the X-ray diffraction analysis. Selected matrices were not water permeable, so there was need for optimization of the matrices water permeability of the three surfactants used for optimization, the optimum surfactant type was anionic Triton H_{66}. This had an influence on the physical properties of the matrices (increase in apparent porosity and water absorption, decrease in bulk density), but were also influenced by the RHA content in the matrices as improvements were mostly noticed in those with RHA than those without. The optimized geopolmer foams was used for MB (10% w/v) removal for 8 hours. Methylene blue removal showed approximately 97% removal efficiency. But this efficiency seem to be dependent on the RHA content, as the matric containing >20% RHA content had a lower efficiency of 95% after 8 hours. Infrared analysis of the membranes used for treatment indicated a new peak at 395 cm^{-1} indicating the absorption of C-N-C of MB. This study had some limitations, which included: Methylene blue removal trials were done for only one concentration. Also, an extensive investigation were not done on the effect of RHA content on the treatment efficiency of the porous geopolymer. Porosimetric analysis were not done on the selected porous geopolymers to determine their pore sizes and types. Furthermore, the membranes were not applied in a real wastewater treatment to determine its potential and efficacy to remove true pollutants from wastewater under different conditions of pH. Nevertheless, this study provides information on some important aspects including: The preferred type of foaming agent to be used and methods to improve pore

uniformity, connectivity, hence improving on the water permeability.

DECLARATION

The authors have no competing interest to declare.

ACKNOWLEDGMENTS

The authors acknowledge the funding of this work from the royal society through the Flair program in mipromala. Part of the analysis for this work was carried out with the support of the department of engineering "Enzo Ferrari" university of Modena.

REFERENCES

1. Abdollahnejad Z, Pacheco-Torgal F, Felix T, Tahri W, Barroso Aguiar J. Mix design, properties and cost analysis of fly ash-based geopolymer foam. Constr Build Mater. 2015;80:18-30.
2. Al Bakri MAM, Kamarudin H, Bnhussain M, Khairul Nizar I, Mastura WIW. Mechanish and chemical reaction of fly ash geopolymer cement-A review. Asian J Sci Res. 2011;1(5):247-253.
3. Bahgat M, Dewedar A, Zayed A. Sand-filters used for wastewater treatment: Buildup and distribution of microorganisms. Water Res 1999;33(8):1949-1955.
4. Bai C, Colombo P. Processing, properties and applications of highly porous geopolymers: A review. Ceram Int. 2018;44(14):16103-16118.
5. Bhuyan MAH, Gebre RK, Finnila MAJ, Illikainen M, Luukkonen T. Preparation of filter by alkali activation of blast furnace slag and its application for dye removal. J Environ Chem Eng. 2021;10(1): 107051.
6. Bragg WH. The structure of magnetite and the spinels. Nature. 1915;95:561.
7. Cheng TW, Lee ML, Ko MS, Ueng TH, Yang SF. The heavy metal adsorption characteristics on metakaolin-based geopolymer. Appl Clay Sci. 2012;56:90-96.
8. Cui Y, Wang D, Zhao J, Li D, Ng S, Rui Y. Effect of calcium stearate based foam stabilizer on pore characteristics and thermal conductivity of geopolymer foam material. J Build Eng. 2018;20:21-29.
9. Davidovits J. Geopolymers and geopolymeric materials. J Therm Anal Calorim. 1989;35:429-441.
10. Downs RT, Palmer DC. The pressure behavior of alpha cristobalite. Am Min. 1994;79(1-2):9-14.
11. Duan P, Yan C, Zhou W, Ren D. Development of fly ash and iron ore tailing based porous geopolymer for removal of Cu(II) from wastewater. Ceram Int. 2016;42(12):13507-13518.
12. Ducman V, Korat L. Characterization of geopolymer fly-ash based foams obtained with the addition of Al powder or H_2O_2 as foaming agents. Mater Charact. 2016;113:207-213.
13. Eliche-Quesada DS, Ruiz-Molina L, Perez-Villarejo E, Castro PJ, Sanchez-Soto. Dust filter of secondary aluminium industry as raw material of geopolymer foams. J Build Eng. 2020;32:101656.
14. Ge Y, Cui X, Kong Y, Li Z, He Y, Zhou Q. Porous geopolymeric spheres for removal of Cu(II) from aqueous solution: Synthesis and evaluation. J Hazard Mater. 2015;283:244-251.
15. Gualtieri AF. Accuracy of XRPD QPA using the combined Rietveld-RIR method. J Appl Crystallogr. 2000;33:267-278.
16. Hajimohammadi A, Ngo T, Mendis P, Kashani A, van Deventer JSJ. Alkali activated slag foams: The effect of the alkali reaction on foam characteristics. J Clean Prod. 2017;147:330-339.
17. Hazen RM, Finger LW, Hemley RJ, Mao HK. High-pressure crystal chemistry and amorphization of α-quartz. Solid State Commun. 1989;72(5):507-511.
18. Heaney PJ, Post JE. Evidence for an I 2/a to imab phase transition in the silica polymorph moganite at ~570 K. Am Min. 2001;86(11-12): 1358-1366.
19. Hirose T, Kihara K, Okuno M, Fujinami S, Shinoda K. X-ray, DTA and Raman studies of monoclinic tridymite and its higher temperature orthorhombic modification with varying temperature. J Mineral Petrol Sci. 2005;100(2):55-69.
20. Yan J, Li R. Simple and low-cost production of magnetite/graphene nanocomposites for heavy metal ions adsorption. Sci Total Environ. 2022;813:152604.
21. Kamseu E, Cannio M, Obonyo EA, Tobias F, Bignozzi MC, Sglavo VM, Leonelli C. Metakaolin-based inorganic polymer composite: Effects of fine aggregate composition and structure on porosity evolution, microstructure and mechanical properties. Cem Concr Compos. 2014;53:258-269.